Time-Domain Characteristics of Slotted-Waveguide Leaky-Wave Antennas

David Kralj and Lawrence Carin, *Senior Member, IEEE*

***Abstract*— A general asymptotic theory is presented to describe the time-domain behavior of leaky transmission lines and antennas. The results are interpreted via a simple geometric construct and data are presented for the particular case of time-domain radiation from a slotted-waveguide antenna. The example data are obtained both experimentally and numerically, with the expected phenomenology demonstrated via time-frequency processing.**

***Index Terms*— Asymptotics, leakage, time domain, time frequency.**

I. Introduction

LEAKY-WAVE antennas [1] and leaky planar transmission lines [2]–[5] have been the interest of extensive research for decades. Recently, there has been significant interest in the characteristics of such devices in the time domain, particularly for high-speed interconnects [6]–[8]. Due to the frequency-dependent group velocities and leakage angles characteristic of most leaky-wave structures, the time- and frequency-domain behavior of such devices are often dramatically different. In this letter, we demonstrate that the time-domain phenomenology characteristic of general leaky structures can be explained in terms of a simple relationship which involves the device geometry and the associated frequency-dependent group velocities and leakage angles of the waves it supports. This understanding is important for the design of time-domain leaky-wave antennas as well as for the avoidance of deleterious effects due to spurious time-domain leakage from printed interconnects [2]–[5]. The time-dependent phenomenology associated with such dispersive structures is demonstrated effectively in the time-frequency phase space [9]–[11]. Example time-frequency results are presented here for the special case of a slotted-waveguide leaky-wave antenna.

II. Analysis

In order that the analysis is presented clearly, we initially consider the specific problem of transient radiation from the slotted-waveguide leaky-wave antenna in Fig. 1, and the results are subsequently generalized. The fields radiated from this antenna can be expressed in terms of the electric vector potential $\boldsymbol{F}(x,y,z,t)$ [12] which, from image theory, is

$$\begin{aligned}\boldsymbol{F}&(x,y,z,t)\\ &= z\frac{-j\epsilon_o}{8\pi}\int_{-\infty}^{\infty} d\omega e^{j(\omega t-\beta z)}\int_{\text{slot}} dx' M_z(x',\omega)\\ &\quad\cdot H_o^{(2)}[\sqrt{k_o^2-\beta^2}\sqrt{(x-x')^2+y^2}]\\ &\approx z\frac{-j\epsilon_o}{8\pi}\sqrt{2j/\pi}\int_{-\infty}^{\infty} d\omega e^{j(\omega t-\beta z)}\int_{\text{slot}} dx' M_z(x',\omega)\\ &\quad\cdot e^{-j\sqrt{k_o^2-\beta^2}\sqrt{(x-x')^2+y^2}}[(k_o^2-\beta^2)((x-x')^2\\ &\quad+y^2)]^{-1/4}\end{aligned} \tag{1}$$

where the x' integral is performed over the slot width, $k_o = \omega/c, c$ is the speed of light in vacuum, M_z is the frequency-dependent slot magnetic current density, β is the frequency-dependent longitudinal wavenumber, and the second equation invokes the large-argument approximation to the Hankel function. The frequency integral in (1) is evaluated using standard asymptotic techniques [13], and therefore we isolate the phase $\exp[j\phi(x,y,z,t;x',\omega)]$, with

$$\begin{aligned}\phi&(x,y,z,t;x',\omega)\\ &= \omega t-\beta z-\sqrt{k_o^2-\beta^2}\sqrt{(x-x')^2+y^2}\end{aligned} \tag{2}$$

and it is assumed that $\exp(j\phi)$ varies with frequency much more rapidly than the other frequency-dependent terms in (1). Using stationary-point asymptotics, we obtain [13]

$$\begin{aligned}F_z(x,y,z,t) &\sim \frac{-j\epsilon_o}{8\pi}\sqrt{2j/\pi}e^{j\pi/4}\int_{\text{slot}} dx'\\ &\quad\cdot\frac{M_z(x',\omega_s)}{[(k_{os}^2-\beta_s^2)((x-x')^2+y^2)]^{1/4}}\\ &\quad\cdot\sqrt{\frac{2\pi}{|\phi''(\omega_s)|}}e^{j\phi(\omega_s)}+\text{c.c.}\end{aligned} \tag{3}$$

where k_{os} and β_s are, respectively, k_o and β evaluated at the stationary-point frequency ω_s, c.c. represents the complex conjugate of the term to its left, and the stationary-point frequency ω_s is determined by solving

$$\begin{aligned}\partial\phi/\partial\omega =& t-z/v_g(\omega)-\csc[\theta(\omega)]\sqrt{(x-x')^2+y^2}/c\\ &-\cot[\theta(\omega)]\sqrt{(x-x')^2+y^2}/v_g(\omega)=0\end{aligned} \tag{4a}$$

or, identically,

$$\begin{aligned}t =& (z-\cot[\theta(\omega_s)]\sqrt{(x-x')^2+y^2})/v_g(\omega_s)\\ &+\csc[\theta(\omega_s)]\sqrt{(x-x')^2+y^2}/c.\end{aligned} \tag{4b}$$

Manuscript received November 7, 1996.

D. Kralj is with the Raytheon Company, Missile Systems Division, Tewksbury, MA USA.

L. Carin is with the Department of Electrical Engineering, Duke University, Durham, NC 27708-0291 USA.

Publisher Item Identifier S 1051-8207(97)03323-0.

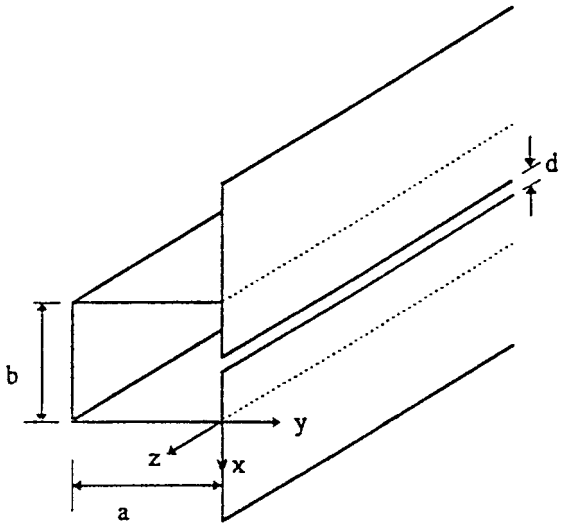

Fig. 1. Slotted-waveguide leaky-wave antenna.

In (3), the "c.c." is present because there are two stationary points, at $\pm\omega_s$. Finally, the frequency-dependent leakage angle [2]–[5] and group velocity are

$$\sin[\theta(\omega)] = \frac{\sqrt{k_o^2 - \beta^2}}{k_o}, \qquad v_g(\omega) = [\partial\beta/\partial\omega]^{-1}. \tag{5}$$

For leaky modes, the wavenumber is complex β [2]–[5], and therefore so too are the leakage angle and group velocity in (5). In most cases, however, the real part of β is much larger than the imaginary part [2]–[5], and therefore the stationary-point frequency can be determined very accurately by using the real parts of $\theta(\omega_s)$ and $v_g(\omega_s)$. The stationary-point condition in (4b) then has the simple geometrical interpretation depicted in Fig. 2 and is summarized here. Assume the transient fields are observed at (x, y, z) and the source is placed at $z = 0$ (the slit starts at $z = 0$). If the frequency component observed at time t is ω_s, then, since it travels at an angle $\theta(\omega_s)$, the fields observed at time t traveled through air a distance $\csc\theta(\omega_s)[(x - x')^2 + y^2]^{1/2}$ from the waveguide slot to the observer. Moreover, from simple geometry, the fields at frequency ω_s traveled down the waveguide a distance $z - \cot(\omega_s)[(x - x')^2 + y^2]^{1/2}$, before being launched (leaked) to the observer. Accounting for the fact that the wave travels at a velocity $v_g(\omega_s)$ along the slot and at a velocity c in air, we arrive at the stationary-point condition in (4b). Thus, the transient fields radiated by the leaky-wave antenna are characterized by a time-dependent instantaneous frequency ω_s, which is dictated by the frequency-domain characteristics of the leakage angle $\theta(\omega)$ and the group velocity $v_g(\omega)$.

Finally, with regard to (4), we see that each source position x' yields a slightly different instantaneous frequency ω_s, and therefore when the total fields are calculated via the integral over the slot width [see (3)], there will be some smearing out of the instantaneous frequency (i.e., at a given time, a *distribution* of instantaneous frequencies will be measured). For narrow slots, however, the change in ω_s caused by variation in x' will be small at most points of observation (x, y, z).

The above analysis focused on transient radiation from a slotted-waveguide leaky-wave antenna. To calculate the time-domain fields *inside* the waveguide, a very similar analysis is utilized, employing the slot magnetic currents and the rectangular-waveguide Green s function [12]. Moreover, the basic ideas and analysis are applicable to time-domain leakage from many other structures of interest, including leakage from microwave interconnects [2]–[5]. For such structures, an expression similar to (1) is obtained [2]–[5], using the more-complicated Green s function characteristic of a layered medium. Additionally, for the case of leakage from an interconnect, the leaked radiation will propagate at an angle into the dielectric substrate and/or into the air [2]–[5], depending on the geometrical configuration and frequency band of interest.

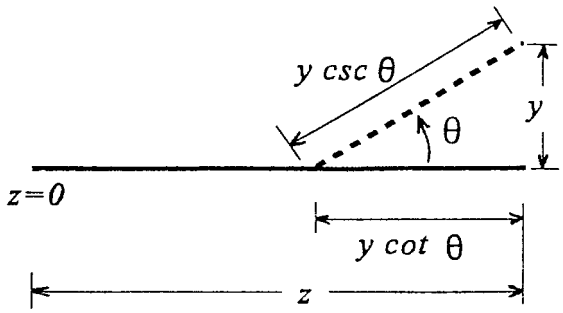

Fig. 2. Schematization of the phenomenology characteristic of time-domain leakage. The radiation is leaked in the form of a cone [2], but for simplicity this figure shows a cut in the (y, z) plane, for $x = x'$ [see (4)].

III. Example Results

To demonstrate the theory outlined above, we consider the slotted waveguide antenna in Fig. 1, with dimensions $a = 0.9$ cm, $b = 1.9$ cm, and $d = 0.2$ cm. This geometry was selected such that the waveguide is largely single moded over the bandwidth of our measurement system [14]. In particular, we have performed measurements using an ultra-wideband, time-domain, optoelectronic system with instantaneous bandwidth from 15 to 75 GHz. In the measurements [14], one antenna was placed inside the slotted waveguide to generate a short burst of electromagnetic radiation and a second antenna was placed inside the waveguide, at a distance $z = 11$ cm from the source antenna. This second antenna measured the time-domain fields, thereby realizing a time-domain S_{21} measurement. The results are plotted in Fig. 3, using the following format. The measured time-domain fields are shown at bottom, the Fourier transform of these fields are shown at left, and the STFT is shown in the center, using a sliding Gaussian window with a 90-ps 3-dB width. In addition to the STFT results (gray scale), the curves in the center of Fig. 3 denote the theoretical instantaneous frequencies predicted by the asymptotic theory in Section II for the TE_{10} and TE_{20} modes (the curves were computed by modifying (2) to $\phi = \omega t - \beta z$, as dictated by the waveguide Green s function, with the frequency-dependent description of β calculated via the Method of Moments (MoM), as discussed below). One notices that there is close agreement between the theoretical (curve) and short-time Fourier transform (STFT)-processed instantaneous frequencies and, as designed in the measurement, only the TE_{10} mode is excited strongly. The significant dispersion characteristic of the slotted waveguide

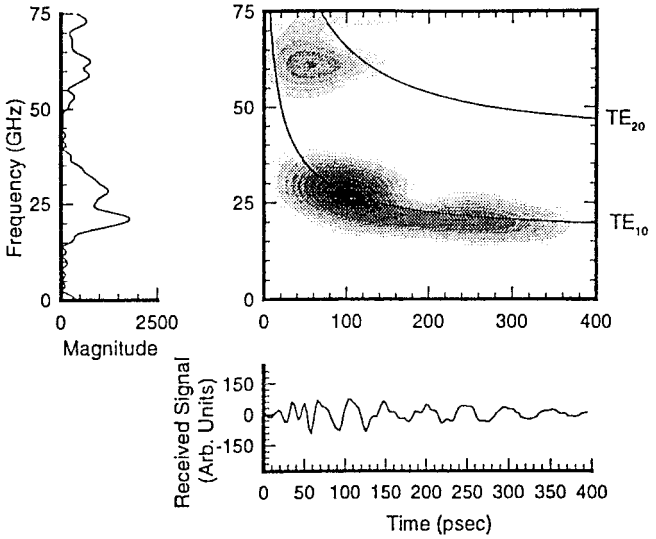

Fig. 3. STFT of the transient fields inside a slotted rectangular waveguide. In the bottom plot are the measured time-domain fields, at left are the Fourier transform of the measured fields, and in the center gray-scale plot the STFT results are depicted. The curves in the center plot are the theoretical instantaneous frequencies predicted by the theory discussed in the text. The incident pulse (not shown) had peak energy around 30 GHz.

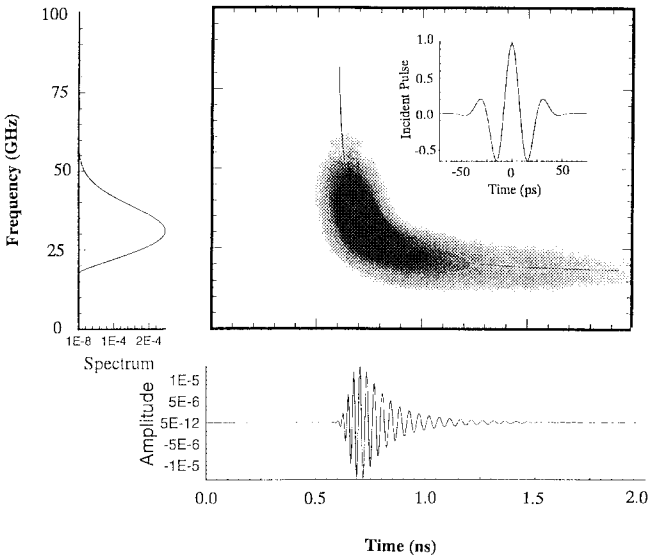

Fig. 4. STFT (center) of the transient fields radiated by a slotted-waveguide antenna. The radiated fields were computed via the MoM using the input pulse at $z = 0$ (shown inset), and the results are plotted using the same format as in Fig. 3. The curve represents the theoretical instantaneous frequencies.

yields an extended (chirped) time-domain response (bottom curve), despite the fact that the initial energy is generated by a short pulse [14].

Our last example considers radiation from the same structure investigated in Fig. 3, with the data generated numerically via the MoM (unlike the fields inside the waveguide, the radiated fields were too weak to measure accurately). In particular, the slot electric fields (magnetic currents) were expanded in a subsectional, pulse basis [15], and the magnetic fields were matched across the aperture, using appropriate Green s functions for the region inside and outside the waveguide. Once the frequency-domain slot magnetic currents were so computed, the radiated fields were calculated using (1), with the inverse Fourier transform performed via a fast Fourier transform (FFT). Further, the MoM results were used to calculate the dispersion properties of $\theta(\omega_s)$ and $v_g(\omega_s)$ in (5), which are needed for computation of the theoretical instantaneous frequencies described in (4).

The time-domain leaked fields were observed at ($x = -0.95, y = 4.5$ cm, $z = 36$ cm), using the input pulse inset in Fig. 4. The results for this case are shown in Fig. 4, employing the same format and time-frequency scheme as in Fig. 3. As in Fig. 3, there is excellent agreement between the time-dependent asymptotic frequencies, denoted by the solid curve, and the time-frequency distribution of the actual radiated fields.

IV. Conclusions

A general and simple asymptotic theory has been presented to describe the properties of leakage in the time domain. The analysis and example results were presented for the particular case of a slotted-waveguide antenna, but it was explained how the results are applicable to a wide class of leaky-wave devices, including leaky interconnects. The theory was successfully compared to measured and numerical data, with the comparison performed in the time-frequency phase space.

References

[1] A. A. Oliner, "Leaky-wave antennas," in *Antenna Engineering Handbook*, R. C. Johnson, Ed. New York: McGraw-Hill, 1993, ch. 10.
[2] D. B. Rutledge, D. P. Neikirk, and D. P. Kasilingam, "Integrated circuit antennas," in *Infrared and Millimeter Waves*, vol. 10, K. J. Button, Ed. New York: Academic, 1983, pp. 1–87.
[3] H. Shigesawa, M. Tsuji, and A. A. Oliner, "Conductor-backed slotline and coplanar waveguide: Dangers and full-wave analyzes," in *1987 IEEE MTT-S Int. Symp. Dig.*, pp. 199–202.
[4] L. Carin and N. K. Das, "Leaky waves on broadside-coupled microstrip," *IEEE Trans. Microwave Theory Tech.*, vol. 40, pp. 58–66, Jan. 1992.
[5] N. K. Das and D. M. Pozar, "Full-wave spectral-domain computation of material, radiation and guided wave losses in infinite multilayered printed transmission lines," *IEEE Trans. Microwave Theory Tech.*, vol. 39, pp. 54–65, Jan. 1991.
[6] T. Leung and C.A. Balanis, "Pulse dispersion in open and shielded lines using the spectral-domain method," *IEEE Trans. Microwave Theory Tech.*, vol. 36, pp. 1223–1226, July 1988.
[7] L. Carin and K. J. Webb, "Isolation effects in single- and dual-plan VLSI interconnects," *IEEE Trans. Microwave Theory Tech.*, vol. 38, pp. 396–404, Jan. 1992.
[8] M. Tsuji and H. Shigesawa, "Packaging of printed circuit lines: A dangerous cause of narrow pulse distortion," *IEEE Trans. Microwave Theory Tech.*, vol. 42, pp. 1784–1790, Sept. 1994.
[9] A. Moghaddar and E. K. Walton, "Time-frequency distribution analysis of scattering from waveguide cavities," *IEEE Trans. Antennas Propagat.*, vol. 41, pp. 677–679, May 1993.
[10] H. Kim and H. Ling, "Wavelet analysis of radar echo from finite size targets," *IEEE Trans. Antennas Propagat.*, vol. 41, pp. 200–207, Feb. 1993.
[11] L. Carin and L. B. Felsen, "Wave-oriented data processing for frequency and time domain scattering by nonuniform truncated array," *IEEE Antennas Propagat. Mag.*, vol. 36, pp. 29–43, June 1994.
[12] C. A. Balanis, *Advanced Engineering Electromagnetics*. New York: Wiley, 1988.
[13] L. B. Felsen and N. Marcuvitz, *Radiation and Scattering of Waves*. Englewood Cliffs, NJ: Prentice-Hall, 1973.
[14] D. Kralj, L. Mei, T.-T. Hsu, and L. Carin, "Short-pulse propagation in a hollow waveguide: Analysis, optoelectronic measurement, and signal processing," *IEEE Trans. Microwave Theory Tech.*, vol. 43, pp. 2144–2150, Sept. 1995
[15] R. F. Harrington, *Field Computation by Moment Methods*. Malabar, FL: Krieger, 1985.